Vol 16 No 7, July 2007
1009-1963/2007/16(07)/2051-05
Chinese Physics
© 2007 Chin. Phys. Soc.
and IOP Publishing Ltd

The increasing of localized free volume in bulk metallic glass under uniaxial compression*

Deng Yu-Fu(邓玉福)†, Yang Fei(杨 飞), Yang Jian-Lin(杨建林), and Zhang Wei(张 微)

College of Physical Science and Technology, Shenyang Normal University, Shenyang 110034, *China*

(Received 10 September 2006; revised manuscript received 16 January 2007)

Using transmission electron microscopy and electron diffraction, we have investigated the microstructure of a $Zr_{55}Al_{10}Ni_5Cu_{30}$ bulk metallic glass under a uniaxial compression until a failure occurs at room temperature. It is shown that the amorphous structure has changed locally in the vicinity of the failure plane after the plastic deformation. An increase in free volume is observed within the localized areas due to the concentration of plastic flow, suggesting that the increasing of local free volume dominates the deformation mechanism of the metallic glass. The effect of free volume on the 'serrated flow' behaviour in the stress–strain curves during the uniaxial compression is discussed.

Keywords: amorphous materials, electron microscopy, plastic deformation, microstructure
PACC: 6140, 6220F, 6116D

1. Introduction

In the last decade, bulk metallic glasses (BMGs) have attracted much attention because of their interesting features and potential applications as structural and functional materials. The deformation behaviours of BMGs have been a hot point of theoretical and experimental investigations.[1−6] It has been universally received that plastic deformation in metallic glasses takes place inhomogeneously due to the formation of the highly localized shear bands at high stresses and low temperatures.[7,8] Some structural changes may occur within the shear bands, causing the local softening or viscosity reduction of the glass. Several theoretical models, such as free volume[3,7−9] and adiabatic heating,[4,6,10] have been proposed to explain the deformation mechanism of the metallic glasses, but there still does not exist a universally receivable view in this respect. In contrast to the fractographic studies of the resulting failure under the different stress conditions by optical micrography and scanning electron microscopy,[11−15] experimental data for structural evolution in BMGs during the deformation are lacking. Thus, it is understandable that the information about the microstructural change induced by plastic deformation in BMGs should be of especial importance for elucidating the deformation mechanism of metallic glasses.

In recent preliminary reports, we have described the high-resolution transmission electron microscopy (HRTEM) observations of voids and nanocrystallization in a BMG fractured by uniaxial compression at room temperature.[16,17] In the present work, we extend the previous studies and attempt to reveal whether and how the microstructural changes can be introduced in a $Zr_{55}Al_{10}Ni_5Cu_{30}$ BMG under uniaxial compression, which serves as part of effort to further understand the deformation mechanism in metallic glasses.

2. Experimental details

The amorphous $Zr_{55}Al_{10}Ni_5Cu_{30}$ rod (in at %) with a diameter of 4 mm and a length of 50 mm was prepared by using the arc-melted mixtures of pure elements in an argon atmosphere and casting into a copper mould. The amorphous structure was identified by x-ray diffractometry (XRD, Rigaku/max-γA diffractometer using Cu Kα radiation, $\lambda = 1.54056$ Å) and transmission electron microscopy (TEM) observations. The uniaxial compressing of the as-cast sample with 4 mm in diameter and 8 mm in length was performed until a failure occurred at a compression rate of 10^{-4} s^{-1} on an MTS 810 testing machine at room temperature. Figure 1 shows the compressive stress–

*Project supported by the National Natural Science Foundation of China (Grant No 10547127) and Experimental Center of Shenyang Normal University, China (Grant No SY-200506).
†Corresponding author. E-mail: yfdeng668@sina.com

strain curve of the $Zr_{55}Al_{10}Ni_5Cu_{30}$ amorphous alloy in an as-cast state. The fracture occurred along the maximum shear plane, which was inclined at about 45° to the compression axis, similar to that in Ref.[12].

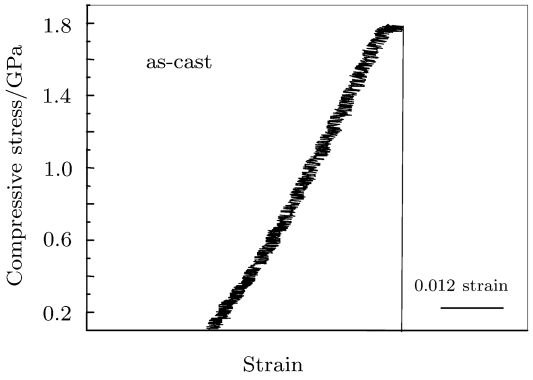


Fig.1. Compressive stress–strain curve of the bulk $Zr_{55}Al_{10}Ni_5Cu_{30}$ amorphous alloy in an as-cast state.

In order to acquire the information about microstructural change in the sample after the failure, we glued two fractured pieces together, and cut the specimens of the metallic glass into a disc with 3 mm in diameter and 600 μm in thickness in the direction perpendicular to the loading axis for TEM observations. TEM specimens were prepared first carefully by the mechanical thinning of the discs to a thickness of 80 μm, and then by the standard twin-jet electrolytic thinning in an $HClO_4$–C_2H_5OH solution (volume ratio 1 : 10) at −25°C, finally by the low-angle (5°) ion milling thinning for about 10 min. The TEM specimens were examined by a JEOL-2010 high-resolution transmission electron microscope operated at 200 kV.

3. Results and discussion

Figure 2 shows the typical XRD pattern obtained from the as-cast amorphous sample, which consists of only one broad amorphous peak with a maximum intensity at the wave vector of 26.2 nm^{-1}. No peaks of any crystalline phases can be seen in the figure, revealing the amorphous structure of the samples.

Figure 3 shows the TEM specimen preparation of the fractured bulk sample. Figure 3(a) is a schematic diagram of the specimen nearby the fracture. The perforation formed after the twin-jet thinning, which is located at nearly 200 μm off the failure plane (dashed line), as indicated by the white arrow in Fig.3(b). Figure 4 is a TEM image of the morphology in the specimen prepared by the twin-jet thinning only. Some void-like regions (VLRs) with nearly rounded morphology with an average size of about 0.7 μm are seen in the specimen. These VLRs are either isolated from or connected with each other, and they distribute inhomogeneously over the whole image. Actually, they are not completely hollow. This result reveals that the local changes of structure occur in our BMG after the plastic deformation, because these regions are preferentially etched during the electrochemical thinning.

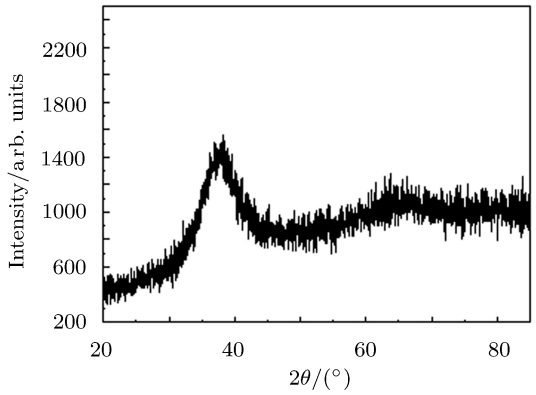


Fig.2. X-ray diffraction pattern of the as-cast bulk $Zr_{55}Al_{10}Ni_5Cu_{30}$ alloy.

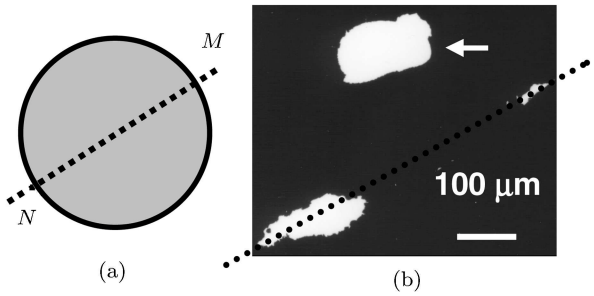


Fig.3. (a) Schematic diagram of the specimen nearby the fracture before the electrochemical thinning. MN is the failure plane. (b) TEM image (lower-magnification) of the specimen after the electrochemical thinning. Perforation (arrowed) formed in the region adjacent to the failure plane (dashed line).

To further shed light on the microstructural changes in the sample, we examined the same specimen followed by the low-angle ion milling. The purpose of this thinning step is to remove the residual chemicals adhering to the specimen surface after the twin-jet thinning, minimizing any possibility of changing the structure induced by ion thinning. The VLRs can still be seen in the specimen as shown in Fig.5(a). Figure 5(b) provides a higher-magnification TEM image of three typical VLRs in the micrograph. The observed contrast is quite different between the edges

of the VLRs, the central regions within the VLRs, and the surrounding matrix. The 'thick' dark areas in and around the VLRs may be due to contamination and/or surface relief of the specimen in the electrochemical thinning. Selected-area electron diffraction (SAED) analyses show that nanocrystallites are formed in the VLR (arrowed). Further discussion on this crystallization can be found in Ref.[17]. Regions outside the VLRs are completely amorphous. However, we cannot obtain any structure information of those 'thick' dark areas from the SAED results.

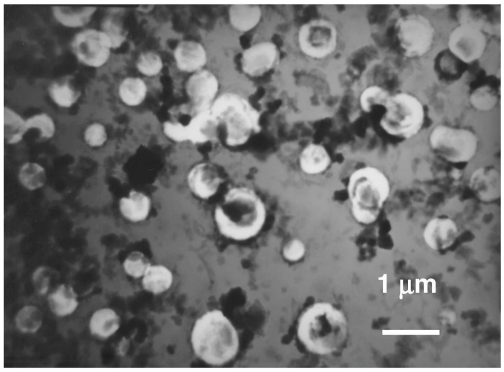


Fig.4. TEM image of the specimen prepared by the twin-jet electrolytic thinning only. The formation of VLRs indicates the local changes in structure due to plastic deformation.

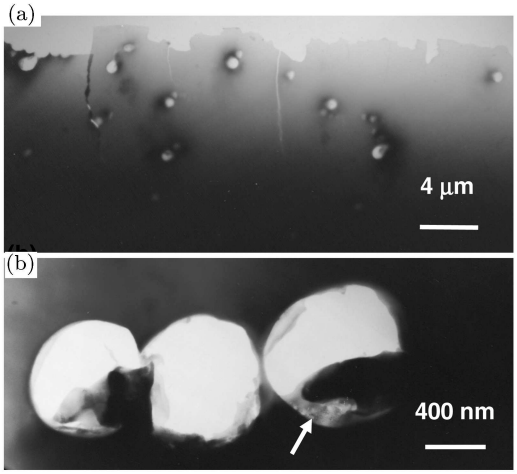


Fig.5. (a) TEM image of the same specimen followed by the low-angle ion milling. (b) A higher-magnification TEM image of the selected area in the specimen. The VLRs can still be seen over the whole micrograph, showing the microstructural changes induced by plastic deformation.

A typical 'thin' region, which may be representative of the different stages of the VLR formation during the electrochemical thinning, is shown in Fig.6(a). It is located on the edge of the perforation created during sample preparation, and has an appearance of meniscus in morphology, and it is lighter in contrast than its surrounding material in the micrograph. Figure 6(b) is the corresponding SAED pattern. Also shown in this figure is the SAED pattern (Fig.6(c)) taken from the surrounding material under the same diffraction conditions, indicating the fully amorphous structure as seen in as-received amorphous material. Although the structure in Fig.6(a) is still in an amorphous state after the plastic deformation, the difference between the two SAED patterns clearly illustrates that the interatomic spacing or free volume increased within the localized 'thin' region associated with shifting toward lower scattering angles and broadening the diffraction halo rings.[17] Figure 7 provides an HRTEM image taken from the region in Fig.6(a). The morphology has an amorphous-like matrix, but contains many medium-range-ordered (MRO) domains (marked by circles) which correspond to local crystalline atomic clusters. Our TEM observations also confirmed that crystallization occurred within this area under the irradiation of electron beam with above a critical current density at room temperature. The details of this electron irradiation-induced crystallization behaviour will be published elsewhere.

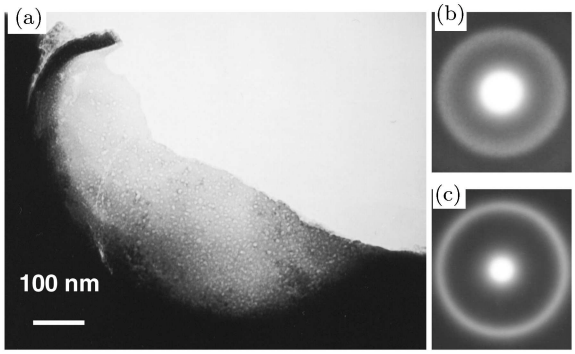


Fig.6. TEM images of a typical 'thin' region (a) and its corresponding SAED pattern (b) and SAED pattern taken from the surrounding material (c), indicating the fully amorphous structure that is not affected by deformation. The broadening and shrinkage of the diffraction halo rings in Fig.6(b) illustrate the increase of free volume within the local region due to the inhomogeneous localization of plastic flow.

To rule out any artifact due to TEM specimen preparation, we have performed a set of observations of the specimens from the bulk as-cast amorphous sample. Figure 8 is a typical TEM image and its corresponding SAED pattern with a diffusive halo ring in the inset. No detectable changes in the microstruc-

ture are observed, although all the TEM specimens were prepared in the same milling conditions. Thus, we conclude that the observed structural characteristic presented in Fig.4 is not produced by an experimental artifact.

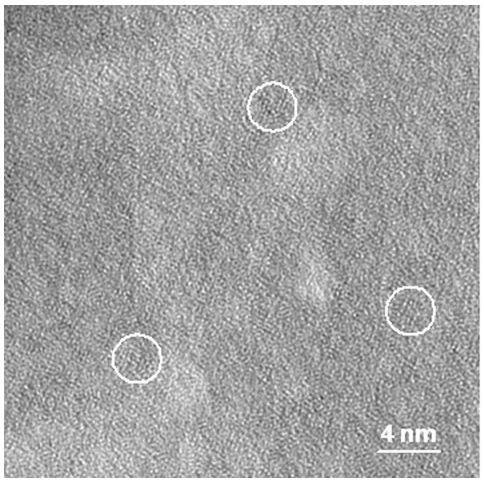


Fig.7. HRTEM image from the region in Fig.6(a). MRO domains are seen in encircled areas.

The basic feature of plastic deformation in metallic glasses is the formation and propagation of localized shear bands. These shear bands formed by both bending and compression are found to be preferentially etched[18−20] and exhibit differences from the undeformed material by the electron diffraction contrast.[21,22] In the present study, however, we do not find any evidence for the shear band formation in the specimen after the plastic deformation. The observations of VLRs (Fig.4) clearly indicate the occurrence of structural changes in our BMG subjected to the macroscopic plastic deformation event. The shrinkage and broadening of diffusive ring pattern (Fig.6(b)) from local deformed areas, give experimental evidence of increasing free volume induced by the localization of plastic flow in the BMG, indicating that the increasing of local free volume dominates the flow process. The magnitude of corresponding scattering vector, defined as $Q = 4\pi \sin\theta/\lambda$ (θ is half the scattering angle and λ the electron wavelength), appears to be significantly smaller in Fig.6(b) than in Fig.6(c), the ratio between them being about 0.87. The VLRs, which may be representative of the shear transformation zones[8] with a higher chemical thinning rate than the surrounding matrix, demonstrate the local softening or density reduction of the glass. This means that localized plastic deformation destroys the chemical short-rang order in the BMG, leading to the formation of a more 'disordered structure'[20,23] within the localized regions where atomic instability and diffusional mobility can become more pronounced than the surrounding amorphous matrix. This result well supports the early experimental observations[8,18,24] and computer simulations,[25] and it is also consistent with the positron annihilation spectroscopy studies.[3]

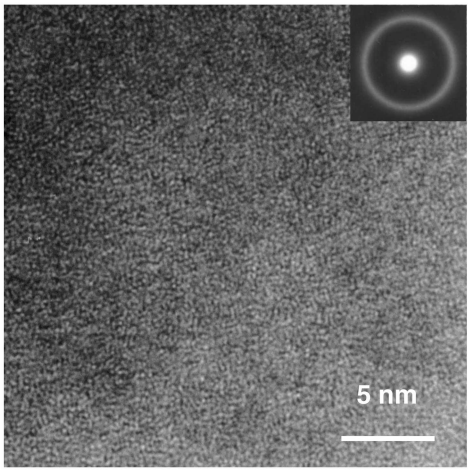


Fig.8. A TEM image and the corresponding SAED pattern (inset) of the bulk $Zr_{55}Al_{10}Ni_5Cu_{30}$ metallic glass, showing the uniform amorphous microstructure of a alloy in an as-cast state.

An attractive phenomenon in the stress–strain curves at a quasi-static strain rate during uniaxial compression is the 'serrated flow' behaviour of metallic glasses.[26] It has been proposed that 'serrated flow' is a consequence of the nucleation of new shear bands or, due to the intermittent slip on previously existing shear bands.[15,19] Although the similar yield drops are observed in the stress–strain curves (not shown here) in this study, no relation between the yield drop and the shear band can be found from our TEM observations on the fractured samples. The structural characteristics observed in the present work strongly suggest that the increase of local free volume induced by the localization of plastic deformation is associated with the 'serrated flow' behaviour during the evolution of deformation.

We now consider a model which is possible to explain the 'serrated flow' in plastic regime under uniaxial compression. Once a metallic glass sample is loaded elastically up to the yielding of stress, the serrated plastic flow takes place, coinciding with the creation of free volume within localized areas due to the concentration of plastic flow. These deformation-induced areas may be initiated individually from various nanometre-scale defects[27] in the metallic glass.

This process may also be dynamic, inhomogeneous, and quantitated, corresponding to the observed multiple serrations. In certain geometries, the number and size of the free volume increasing sites within each single serration appear to reach a saturated point or critical value related to the applied stress conditions, as characterized by repeating cycles of a sudden stress drop followed by elastically reloading in the stress-strain curves. The fact that the failure strain decreases and the amplitude of 'serrated flow' diminishes with the increase of strain rate[5,28] is properly due to the influence of loading rate on the initiation and propagation of local free volume. Namely, a rapid and continuous increase in free volume may occur at higher strain rates, resulting in the diminishment of 'serrated flow' within the spatiotemporal resolution of the observations, and a limited plasticity as well as lower strength. When the stress concentration is large enough, the rapid development and propagation of local free volume may create a catastrophic softening layer along a maximal shear stress plane where the failure occurs eventually. In particular, the effect of adiabatic heating caused by work done on the sample may occur mainly in the maximal shear plane at the moment when the final fracture event happens as the evidence of the molten droplets observed on the fracture surface[4,26] and the emission of visible light recorded using high-speed cinematography.[5]

4. Conclusions

The microstructural changes induced by plastic deformation are observed in the $Zr_{55}Al_{10}$ Ni_5Cu_{30} BMG under uniaxial compression at room temperature. Electron diffraction analysis and TEM observations give experimental evidence of the increase of free volume within the locally of deformed areas due to the localization of plastic flow, suggesting that the increasing of free volume is a dominant deformation mechanism of metallic glasses. 'Serrated flow' behaviour in the stress–strain curves under uniaxial compression is considered to arise from the formation and propagation of local free volume during the plastic deformation.

Acknowledgement

The authors are grateful to Dr Q. S. Zhang for assistance with the quasi-static compression experiments and sample preparation. Part of this work was performed at the Shenyang National Laboratory for Materials Science, Institute of Metal Research, Chinese Academy of Sciences.

References

[1] Zhao Z F, Zhang Z, Li Z, Wen P, Zhao D Q, Pan M X, Wang W L and Wang W H 2004 *Acta Phys. Sin* **53** 850 (in Chinese)
[2] Meng Q G, Li J G and Zhou J K 2006 *Chin. Phys.* **15** 1549
[3] Flores K M, Suh D, Dauskardt R H, Asoka-Kumar P, Sterne P A and Howell R H 2002 *J. Mater. Res.* **17** 1153
[4] Liu C T, Heatherly L, Easton D S, Carmichael C A, Schneibel J H, Chen C H, Wright J L, Yoo M H, Horton J A and Inoue A 1998 *Metall. Mater. Trans.* A **29** 1811
[5] Hufnagel T C, Jiao T, Li Y, Xing L Q and Ramesh K T 2002 *J. Mater. Res.* **17** 1441
[6] Bruck H A, Rosakis A J and Johnson W L 1996 *J. Mater. Res.* **11** 503
[7] Spaepen F 1977 *Acta Metall.* **25** 407
[8] Argon A S 1979 *Acta Metall.* **27** 47
[9] Steif P S, Spaepen F and Hutchinson J W 1982 *Acta Metall.* **30** 447
[10] Leamy H J, Chen H S and Wang T T 1972 *Metall. Trans.* **3** 699
[11] Yoshimi K, Kato H and Inoue A 2005 *Mater. Trans.* **46** 2870
[12] Bengus V Z, Tabachnikova E D, Miskuf J, Csach K, Ocelik V, Johnson W L and Molokanov V V 2000 *J. Mater. Sci.* **35** 4449
[13] Conner R D, Rosakis A J, Johnson W L and Owen D M 1997 *Scripta Mater.* **37** 1373
[14] Liu L F, Dai L H, Bai Y L, Wei B C and Echert J 2006 *J. Mater. Res.* **21** 153
[15] Hufnagel T C, EI-Deiry P and Vinci R P 2000 *Scripta Mater.* **43** 1071
[16] Deng Y F, He L L, Zhang Q S, Zhang H F and Ye H Q 2003 *Adv. Eng. Mater.* **5** 738
[17] Deng Y F, He L L, Zhang Q S, Zhang H F and Ye H Q 2004 *Ultromicroscopy* **98/2-4** 201
[18] Pampillo C A and Chen H S 1974 *Mater. Sci. Eng.* **13** 181
[19] [Pampillo C A 1975 *J. Mater. Sci.* **10** 1194
[20] Pampillo C A 1972 *Scripta Metall.* **6** 915
[21] Donovan P E and Stobbs W M 1981 *Acta Metall.* **29** 1419
[22] Pekarskaya E, Kim C P and Johnson W L 2001 *J. Mater. Res.* **16** 2513
[23] Polk D E and Turnbull D 1972 *Acta Metall.* **20** 493
[24] Takayama S and Maddin R 1976 *Metall. Trans.* A **7** 1065
[25] Maeda K and Takeuchi S 1981 *Phil. Mag.* A **44** 643
[26] Wright W J, Schwarz R B and Nix W D 2001 *Mater. Sci. Eng.* A **319–321** 229
[27] Li J, Wang Z L and Hufnagel T C 2002 *Phys. Rev.* B **65** 144201
[28] Mukai T, Nieh T G, Kawamura Y, Inoue A and Higashi K 2002 *Intermetallics* **10** 1071